ELECTRON IMPACT IONIZATION

For atoms and molecules the term *electron impact ionization* applies to the process in which one or more electrons bound to a target are removed as a result of collisions between a

free energetic electron and a target atom or molecule, thereby leaving the target species positively charged. The various processes, among many others, that may take place as a result of collision can be represented by the following relations:

$$e^-(E_0) + A \Rightarrow A^{n+} + (n+1)e^-(E_o - E_i) \quad (1)$$

or

$$e^- + MN \Rightarrow MN^{n+} + (n+1)e^- \quad (2)$$

$$\Rightarrow M^+ + N \text{ or } M + N^+ \quad (3)$$

$$\Rightarrow M^+ + N^- \text{ or } M^- + N^+ \quad (4)$$

where A is an atomic species and MN a molecule with atomic and/or molecular components M and N, e^- an electron, E_0 the kinetic energy of the incident electron, and n is the degree of ionization.

The efficiency with which a projectile can remove bound electrons from a target is related to a quantity commonly called *cross section* and has the dimensions of area and is expressed in units of m^2 (square meters). Its value mainly depends on the atomic and molecular structure of the target species and kinetic energy of the incident electron.

The cross section represented by Eqs. (1) and (2) are traditionally called *direct ionization* or multiple ionization. Those represented by Eqs. (2), (3), and (4) are called direct or partial and dissociative ionization cross sections, respectively (conventionally represented by symbols σ_p and σ_d, respectively). A sum of all cross sections for one species is called the total ionization cross section of that species and is represented by the symbol

$$\sigma_T = \sigma_p + \sigma_d \quad (5)$$

It will be explained in the following paragraphs that the ionization cross sections for a specific species can be obtained either by measuring the ion current or by counting each individual ion when the number of ions produced as a result of collision is very small. If the ions are counted instead of integrated, then the total ionization cross section is called the *total counting ionization cross section,* σ_c, and is represented by the following relation:

$$\sigma_c = \sum_p \sigma_p + \sum_{i,n} \sigma_{i,n} \quad (6)$$

where p refers to the direct ionization process [Eq. (2)] for the removal of one or more electrons from the target, n is the degree of ionization of the dissociated ion, and i identifies the species resulting from the dissociation of the molecule. When the total ion current is measured for obtaining the cross section it is commonly called the *gross ionization cross section,* σ_g, and is represented by the following equation:

$$\sigma_g = \sum_p \sigma_p + \sum_{i,n} Z_i \sigma_{i,n} \quad (7)$$

where Z_i is the degree of ionization of the ith species and other symbols have been defined in previous paragraphs.

Cross-section values are important for understanding properties of various plasmas (1). Their values are important for calculating abundances of elements observed in astrophysical plasmas and for the interpretation of mass spectrometric data. Nowadays, low-temperature plasmas are being extensively employed for processing semiconductors. Properties of the ionosphere of planets, comets, and Earth can be better understood with the knowledge of electron-impact cross sections. They are also important for calculating the penetration depths of β particles in biological samples.

The values of cross sections for a species are important and must be accurately known for some applications. Their values can be obtained either by theoretical calculations or experimental techniques. It has been found that simple classical methods (1) of calculating cross sections do not predict their values accurately. Therefore, quantum-mechanical calculations (2) are employed, which are difficult because the two free electrons require continuum wave functions. The calculations involve coupled differential equations. Because of many-body interactions occurring in these calculations they tend to be very complicated. Several methods of approximations (3) have been developed in the past to make the calculations simple yet predict fairly accurate values. Therefore, semiempirical methods have also been developed. According to one semiempirical classical calculation [Lotz formulas (4)] the ionization cross sections can be calculated from the following formula:

$$\sigma_I = \sum_{n=1}^{Ns} \zeta_n (a \ln u / E_0 I_n) \quad (8)$$

where ζ_n is the number of equivalent electrons in the nth subshell, $a = 4.5 \times 10^{-14}$ eV^2, $u = E_0/I_n$ is the reduced energy of the impacting electron, I_n is the binding energy of electrons in the nth subshell, and $\ln(u)$ is the logarithm of the reduced energy u.

Although cross-section values have been measured since the 1920s, the available data until 1950 were for simple and benign gases such as hydrogen, nitrogen, and oxygen. In the 1950s the activity related to measuring cross sections was dormant. However, in the 1960s, due to interest in lasers and fusion plasmas, the field revived and several groups (e.g., 5,6) designed and fabricated new instruments to carry out measurements of cross sections.

MEASUREMENT OF CROSS SECTIONS

There are different versions of experimental apparatus employed by various researchers for the measurement of cross sections. However, conceptually, most of them consist of components shown in Fig. 1. Each component will be briefly described here and references will be given for detailed understanding.

Electron Gun

The electron gun produces a collimated beam of electrons, the kinetic energy of which can be varied or fixed. There are several different designs of an electron gun (7,8). The simplest one uses a tungsten hairpin filament that can be heated in a vacuum to produce electrons. The electrons boil off the filament in the form of a cloud. The cloud consists of electrons that have an energy spread ΔE. This spread is related to the temperature of the filament (9). Therefore, the temperature of the filament plays an important role in determining the

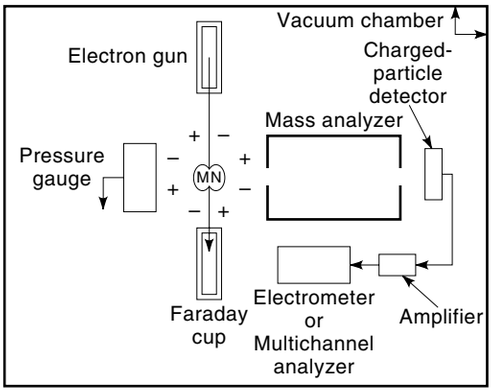

Figure 1. A conceptual diagram of the experimental arrangement commonly used in ionization studies.

energy spread of the electrons. The cooler the filament, the smaller the energy spread. However, recently it has been shown (8) that the material of the filament is also important. Filaments made of irridium have less spread than the filaments made of tungsten. For most experiments smaller values of ΔE are desirable.

The electrons are subsequently collimated to form a beam. In general, two methods have been employed for collimating them. They are (1) the electrostatic method (8) and (2) the magnetic method (7). In the electrostatic method the cloud of electrons is pulled away from the filament region and converted into a beam by a series of electrostatic lenses to form a beam (7,8). A simple arrangement of lenses is shown in Fig. 2. The energy of the electron beam is determined by the potential difference between the filament and ground of the system.

The magnetic collimation is based on the fact that electrons follow the magnetic lines of force in helical paths. In a magnetic electron gun the electron cloud is pulled away from the filament region in the same way as in the electrostatic gun and is subsequently directed along the axis of the electron gun. A magnetic field is applied along the axis of the gun. Figure 3 shows a simple design (10) of an electron gun that uses magnetic collimation. In this case the magnetic field is produced by a solenoid constructed of vacuum-compatible materials.

The previously described simple electron guns (electrostatic or magnetic) generate electron beams with energy spreads varying from about 0.25 eV to 0.5 eV. Lower-energy spreads can be achieved by passing the electron beam

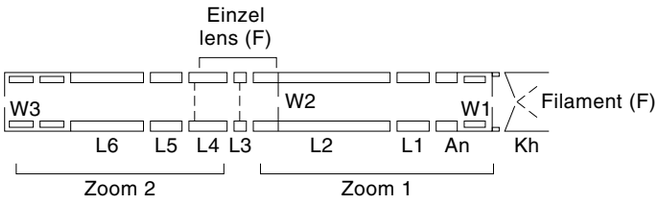

Figure 2. A simple electrostatic electron gun. The electrons are extracted from the filament region by lens W1. They are then collimated and accelerated by an Einzel lens and focused at the exit aperture of lens W3.

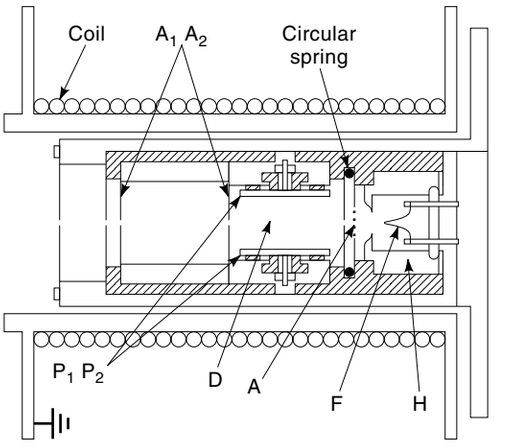

Figure 3. A simple magnetically collimated electron gun. The coil produces axial magnetic field. F, the filament; H, the cathode housing; A, the aperture for collimating electrons; D, deflectors for deflecting the electron beam; P_1 and P_2, deflector plates; A_1 and A_2, apertures.

through an energy-dispersive device. There are several different types of dispersive devices (11). Dispersion in magnetically collimated beams is achieved by passing them through a region of crossed electric and magnetic fields. The electron guns that employ this principle of dispersion are called *trochoidal monochromators.* There are several designs of these monochromators. Reference 12 and references contained therein will provide a good understanding of the design principles.

Faraday Cup

The beam of electrons, after leaving the electron gun, is made to collide with the target species under study. As a result of collisions, ions are produced and colliding electrons get deflected from their original path. Those electrons that do not collide with the target species keep on going on their path and are collected by a device called a Faraday cup, cylinder, or cage. The first description of this device dates back to 1895 (13), 1896 (14), and 1897 (15). The main requirement in designing these devices is that they should be able to collect all electrons without returning them back to the collision region. Figure 4(a) shows the simplest design used by Perrin (13). Figure 4(b) shows a design, used in the author's laboratory, along with its wiring diagram.

Ion Source

As mentioned before, the beam of electrons is passed through the target species, the cross sections of which need to be measured. These target species can be generated by filling the entire vacuum chamber with the gas under study. As shown in Fig. 1, the region between the electron gun and Faraday cup becomes a source of ions. Therefore, this region is generally called the *ion source.*

Instead of filling the entire chamber with gas the target species can also be generated in the form of a beam of atoms or molecules. In the case of gases a beam can be easily generated by flowing the gas through a capillary tube. For solids the material in the form of powder is filled inside a crucible that can be heated by electron bombardment or the resistive

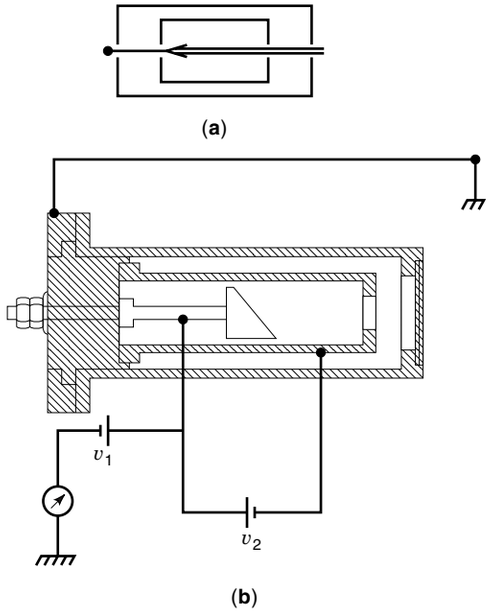

Figure 4. (a) Perrin's Faraday cup. (b) A schematic diagram of the Faraday cup used in the author's laboratory.

heating (16) method with a fine hole at the top through which the vapor of the sample efusses. Figure 5 shows a schematic diagram of the crucible used in the past by the author (11,17) for forming the beams of solid materials. If the target species of interest is in the form of a liquid (18) at normal temperature and pressure, then the liquid is usually filled inside a glass bulb that is heated to vaporize the material. The vapor is subsequently allowed to effuse through a hypodermic needle to form a beam.

When the beam of electrons is made to collide with the target species by passing the electron beam through the gas-filled vacuum chamber, the experimental arrangement is called the *static gas* collision geometry. In the case in which the target species is prepared in the form of a beam, then it is called the *beam-beam* or *crossed-beam* collision geometry.

Ions produced as a result of collisions in the ion source are extracted by an ion extraction system. There are several methods of ion extraction (19). The ion current is usually measured by a sensitive electrometer that can detect currents in the picoampere range. For very weak currents the ions are counted individually. For this purpose, each individual ion is detected by a charged-particle detector (usually called a channeltron, spiraltron, or channel plate) that multiplies the charge of each ion by a factor of about 10 (20). Thus each ion is converted into a current pulse that is subsequently amplified by a fast electronic amplifier. The amplifier gives rise to a pulse of about 5 V amplitude corresponding to each detected ion. Each pulse is stored in the memory of a device called a *multichannel* analyzer as a function of electron-beam energy. The number of pulses counted per second is a measure of ionization current, which is directly proportional to the cross section. By varying the energy of the electron beam and counting the ions for each energy a plot is made between the count rate and electron-impact energy. A typical plot is shown in Fig. 6. Since this plot represents the efficiency with which ions are formed as a function of electron-impact energy, it is generally referred to as the *ionization efficiency curve.* It also represents the dependence of cross sections on the electron energy for the atom or molecule under study.

If all ions produced in the ion source are collected from the ionization region, then the ionization cross section derived from this measurement is called total ionization cross section σ_c or σ_g as defined by Eqs. (6) or (7), respectively. The total ion current I_T (total current generated by all ionic species irrespective of their degree of ionization) can be related to various measurable parameters through the following relation:

$$I_T = N_n \sigma_g L I_e \tag{9}$$

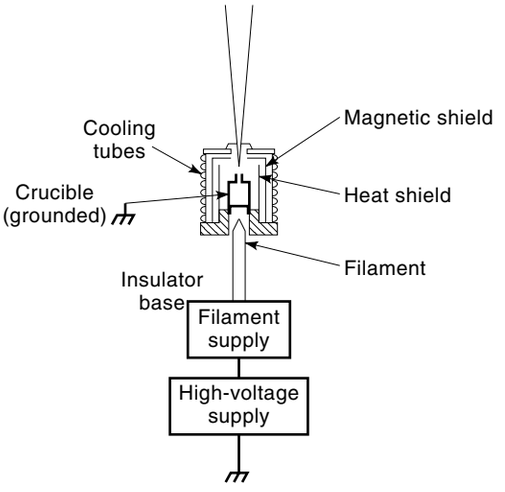

Figure 5. Schematic diagram of a high-temperature crucible used for forming beams of metal atoms.

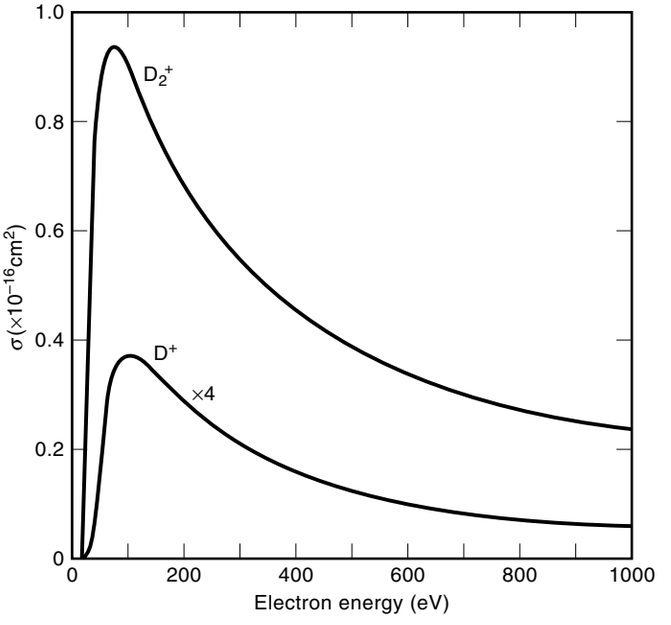

Figure 6. Typical ionization efficiency curves (shown by a solid line). The ionization current is directly proportional to cross sections.

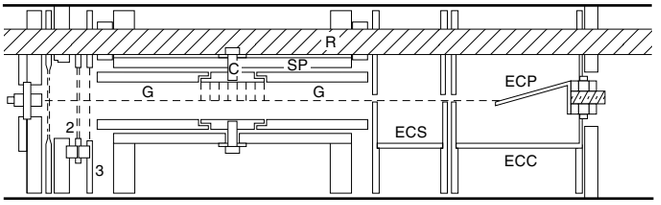

Figure 7. Apparatus used by Rapp and his associates for the measurement of absolute values of cross sections for a number of atmospherically important atoms and molecules.

where N_n is the number density of the target species, L the path length (for the case of static gas collision geometry) of the electron beam in the gas under study, and I_e is the current of the electron beam.

Equation (9) is used for measuring absolute values of cross sections σ_g. For this purpose one has to measure absolute values of all other quantities shown in Eq. (9). N_n can be obtained by measuring the gas pressure in the ion source under study, L can usually be accurately obtained by a calibration procedure employing a gas the cross sections of which are accurately known, and I_e is measured by the Faraday cup.

By utilizing the static gas geometry Rapp, Englander-Golden, and Briglia (5) measured accurate values of cross sections for a number of atmospherically important gases in 1965. Their apparatus is shown in Fig. 7. Instead of a hairpin filament they used an oxide-coated cathode as a source of electrons. Their method was to obtain relative values of cross sections first at different electron-impact energies by plotting the ionization efficiency curves. Then at a fixed electron-impact energy absolute cross sections were obtained by measuring all quantities of Eq. (9).

For the case of crossed-beam collision geometry the relationship between the ion current and cross section is not so simple as in Eq. (9). It is then written (21) as

$$I_m(E_0) = K(m)\sigma_m(E_0)\int_v f(r, E_0)\rho[r]\Delta\Omega[r]\,dr \qquad (10)$$

where $I_m(E_0)$ is the ion current of mass m, $K(m)$ is the mass-dependent transmission efficiency (19) of the ion extraction and detection system, $\sigma_m(E_0)$ is the value of the cross section for ions of mass m as a function of the electron-impact energy E_0, $\rho[r]$ and $\Delta\Omega[r]$ are, respectively, the target density and the solid angle subtended by the detector optics at a point r within the collision volume v, and $f(r, E_0)$ is a function of r and electron-impact energy (see Ref. 21). It is clear from Eq. (10) that accurate measurement of each and every quantity shown on the right-hand side of this equation is a very difficult task. Therefore, the crossed-beam collision geometry is not quite suitable for the measurement of absolute values of cross sections.

Mass Selectors

As a result of the dissociation of molecules, atomic and molecular species in their various ionic states are produced [Eqs. (3) and (4)]. For measuring cross sections for dissociative and multiple ionization processes a mass spectrometer is required for selecting a particular species of interest. A mass spectrometer actually measures the mass-to-charge ratio of an ion. Thus, it also distinguishes between the various multiply charged ions.

Measurement Procedure

The procedure for the measurement of cross sections normally proceeds through the following steps (5): (1) The energy E_0 of the electron beam is fixed, (2) ions of specific mass-to-charge ratio are extracted out of the collision region and the ion current is recorded by an electrometer, (3) for the static gas collision geometry pressure of the gas under study and the electron-beam current is measured. These quantities are substituted in Eq. (9) and the value of the cross section is calculated.

In the procedure for measuring cross sections by utilizing the crossed-beam collision geometry, the measurement of absolute values of quantities on the right-hand side of Eq. (10) is very difficult to obtain with any accuracy. Therefore, the measured cross section is highly unreliable due to following reasons: (1) A reliable estimate of the number density of the target species is very difficult with any accuracy, (2) the length L is almost impossible to measure, and (3) estimation of the size of the collision volume is highly unreliable due to uncertainty in the estimation of the part of the electron beam which actually interacts with the target. However, there are certain advantages of the crossed-beam collision geometry. The main advantage is that it presents a very well-defined ion source to the mass spectrometer and collection of all ions is possible.

In the procedure for measuring cross sections by utilizing the crossed-beam collision geometry, the following steps are taken: (1) The electron-beam energy is varied continuously and the ion current is recorded as a function of electron beam energy E_0. As explained in previous paragraphs the resulting plot is the ionization efficiency curve. (2) The next step is to normalize this curve by a known value of cross section. Therefore, if an absolute value of a cross section is available at one point of this plot, then the entire plot can be normalized to yield cross-section values at other electron-impact energies. There are several procedures of normalization. One of them was developed in the author's laboratory by utilizing a method called *the relative flow technique* (20,22). This technique is applicable only to those species that are in a gaseous form or vapor state at normal room temperature and pressure.

The relative flow technique depends on the fact that if a gas flows through a capillary tube and if the flow rate is very small, then the flow rate can be related to the spatial and velocity distribution of molecules in the beam (21). Thus, if a gas for which the cross sections are not known flows through a capillary tube and if we measure the ion current $I_u(E_0)$, then it can be related to unknown quantities shown on the right-hand side of Eq. (10). Subsequently, if we stop the flow of this gas through the capillary tube and start the flow of a gas (such as He) the cross sections of which are accurately known in such small quantities that the electron-beam current and other experimental conditions do not change then the ion current, I_s, for this gas will also be given by Eq. (10). We can relate the two ion currents, I_s and I_u, through the following equation:

$$\sigma_u(E_o) = \sigma_s(E_o)[I_u(E_o)/I_s(E_o)](M_s/M_u)^{1/2}\,(F_s/F_u)[K(m_s)/K(m_u)] \qquad (11)$$

where the index u stands for a gas whose cross sections are unknown and s represents a standard gas, such as He, the cross sections of which are accurately known. $K(m_s)$ and $K(m_u)$ are the mass-dependent transmission and detection efficiency (23) of the apparatus. M_s and M_u are the molecular weights of the standard gas and the gas under investigation, respectively. F_s and F_u are the flow rates of the standard gas and the gas for which cross sections are not known, respectively. Various experimental details of the relative flow technique can be found in several publications (e.g., Refs. 20 and 22).

IONIZATION PROPERTIES OF RADICALS AND EXCITED STATES

Studies related to stable species are readily available in the previously published literature. However, the same is not true for radical species. This is due to the fact that radical species are difficult to prepare in the form of a target and are short-lived. For example, species such as O, N, and C are difficult to generate in the form of a beam. Pioneering work in this area has been done by Hays et al. (24) and subsequently by Deutsch, Becker, and Mark (25). The apparatus of Hays et al. is shown in Fig. 8. In this apparatus the beam of radical species is prepared by forming a beam of ions of the species under study such as N^+. This beam is accelerated to high energies and is then passed through a cell filled with the vapor of an appropriate material such as alkali-metal atoms. In the cell charge-exchange reactions take place, and a fast neutral beam of atoms emerges. This beam is then employed as the target beam for colliding an energy-selected beam of electrons.

POLAR DISSOCIATION

Equation (4) shows a situation in which the molecule dissociates into two component ions: one positive ion and one negative ion. This process is called *ion pair formation* or *polar dissociation.* This type of dissociation takes place through molecular states that are Coulombic (26) in nature. Negative ions are generally formed by the process of dissociative attachment. Figure 9 shows a graph of O^- intensity resulting from low-energy electron collisions with CO. The first spectral feature is O^- formed by dissociative attachment. However, at higher impact energies the curve slowly rises above the background and goes through a maximum just like the ionization efficiency curves shown in Fig. 6. The continuum part of this curve represents the process of polar dissociation in CO.

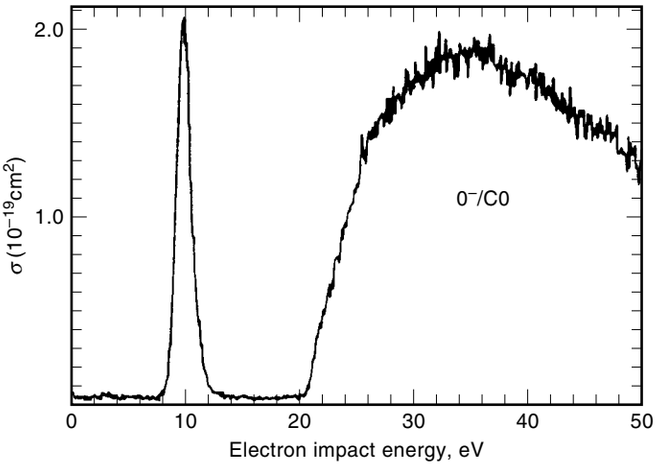

Figure 9. Dissociative attachment and polar dissociation cross sections for the production of O^- from CO.

Ionic states are formed when two oppositely charged species are brought close to each other. The two charges experience the Coulomb force. Figure 10 shows typical curves con-

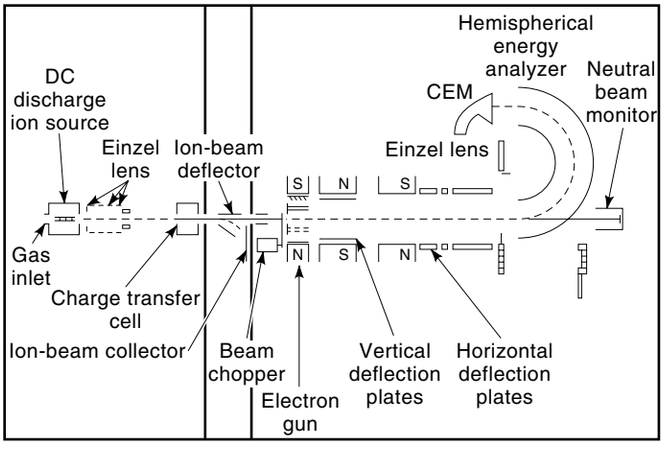

Figure 8. A schematic diagram of the apparatus used by Hays et al. (24) for the measurement of cross sections of radical species.

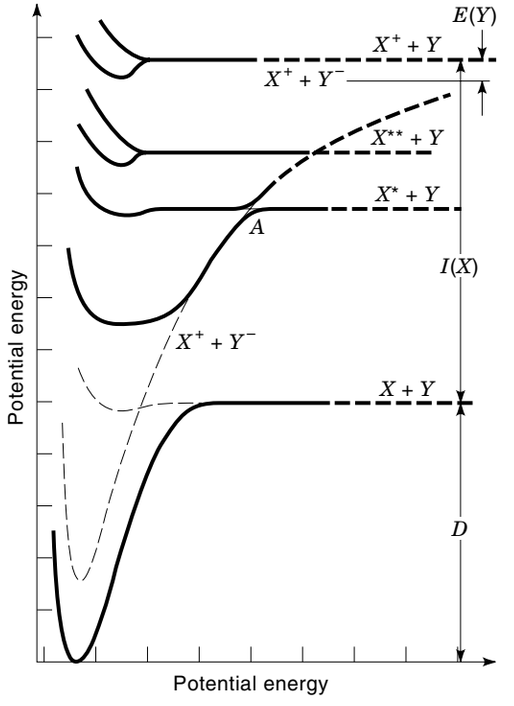

Figure 10. Typical potential energy curves which give rise to polar dissociation in molecules.

structed from a potential of the following form:

$$V = -k_e(e^2/r) + Be^{-r/\rho} \tag{12}$$

These curves are generally crossed by (in the zero-order approximation) a number of their covalent excited states. These covalent states are essentially flat at large nuclear distances. Because the ion-pair formation takes place through the dissociation of neutral states of a molecule, positive ions begin to appear at energies lower than the ionization potential of the molecule.

DISSOCIATION OF MOLECULES INTO NEUTRAL SPECIES

Equation (4) represents dissociation of a molecule into a pair of ions. However, dissociation of a molecule into neutral fragments is a process of great interest to the subject of plasma chemistry. For example, $e^- + N_2 \Rightarrow N + N$ is a very important process for the Earth's atmosphere. However, reliable experimental values for this process are not known. The main difficulty is due to the fact that methods to detect neutral fragments are difficult to implement. Methods such as laser-induced fluorescence (27) (LIF) and multiphoton ionization (MPI) are being developed, but both methods are either very selective or difficult to implement. Therefore, data on the production of neutral fragments by electron impacts on molecules are scarce at the present time.

A method that has been pioneered by Winters and Inokuti (28) utilizes the technique of trapping of the neutral species from which one can infer the intensity of the species produced as a result of electron impact. More recently Goto et al. (29) have reported an experimental apparatus that is capable of measuring cross sections for the production of neutral particles. The apparatus is a dual-electron-beam device that is combined with a quadrupole mass spectrometer. This system consists of three compartments that are differentially pumped. The first compartment is a dissociation cell in which a primary electron beam dissociates the molecule of interest. The second compartment is a detection cell in which a probing electron beam (10 eV to 25 eV energy) emitted from a rhenium filament selectively ionizes neutral radicals that effuse from the first cell through a 4 mm diameter hole into the ionization chamber.

As mentioned before, lasers have also been employed for detecting neutral fragments. It utilizes a tunable dye laser, which, when tuned to correct frequencies, produces fluorescence signal from the neutral particles. The technique is known as LIF. Although LIF is a powerful tool for detecting certain species, its implementation is extremely difficult and works only for those species that strongly absorb laser radiation in the wavelength range that the tunable dye laser can produce.

IONIZATION PROPERTIES AT THE THRESHOLD OF IONIZATION

The threshold ionization (30) potential can be defined as the electron-impact energy at which ionic species in the target begins to appear. The energy at which it begins to appear is generally called *appearance energy* or *appearance potential* (30). In Fig. 6 an ionization efficiency curve near the threshold of ionization of acetylene is shown. The point where the curve begins to rise above the background is used to calculate the appearance potential of the species.

The ionization efficiency curve in the neighborhood of the ionization potential is of interest because it is the region where for many species autoionization states are present. It is also the region that lies at the interface of classical mechanics and quantum mechanics.

A relationship that is well known in atomic physics for ionization is called the Wannier (31) law. It describes the dependence of cross sections on excess electron-impact energy $(E_0 - E_i)$:

$$\sigma_p \propto (E_0 - E_i)^{1.127} \tag{13}$$

where E_0 is the electron-impact energy and E_i is the ionization potential of the target species. This equation does not provide any information on how far above the ionization threshold this law is applicable.

The ionization threshold region can be studied by photoabsorption as well as by electron-impact ionization. The photoabsorption method is superior to the electron-impact method from the point of view of high resolution, but in the latter case the resolution is poor. Therefore, the ionization potentials derived from photoabsorption data are considered to be more accurate than those obtained from electron impact. However, electron impact can excite all energy levels of the target near the threshold of ionization. Therefore, by electron impact one can probe those states of the target that are optically forbidden.

ADDITIVITY RULE

Owing to complications related to many components present in a large molecule, theoretical calculations are very difficult. However, cross sections for ionization of large molecules can be "roughly" estimated by the application of the additivity rule (32). According to this rule the cross section of a molecule can be estimated by summing up cross sections of individual atomic and molecular components of the molecule. Thus, a cross section for a molecule MNP can be roughly estimated by summing individual cross sections for M, N, and P, i.e., $\sigma_{MNP} = \sigma_M + \sigma_N + \sigma_P$, where σ_{MNP} is the total ionization cross section for the production of MNP^+ from MNP, σ_C is the cross section for the ionization of the C atom, and σ_O is the ionization cross section of the O atom. It was shown by Grosse and Bothe (32) and more recently by Orient and Srivastava (33) that this rule works well for organic molecules and for high electron-impact energies. Substantial progress in the application of the additivity rule has been made recently by Becker and his group (34).

In general, almost all ionization curves (Fig. 6) have one common feature: they slowly rise above the background at the threshold of ionization, go through a maximum value, and then slowly fall to small values at higher electron-impact energies. The peak value of cross sections usually lies in the range of about 75 eV to 100 eV for most species. Franko and Daltabuit (35) have derived an empirical relation among the maximum value of ionization cross section, the energy at

which it is maximum, and its ionization potential:

$$\sigma_{max} u_{max} = \text{const} \times \zeta (R/I)^2 \tag{14}$$

where $u = E_0/I$, I being the ionization potential of the atom, and ζ is the number of equivalent electrons in the outer shell.

KINETIC ENERGIES OF THE FRAGMENT IONS

It was first pointed out by Rapp, Englander-Golden, and Briglia (5) that molecular dissociation gives rise to energetic ions. The ions are created with energies ranging from almost 0 eV to larger values. These energetic ions can give rise to a wide variety of chemical reactions in a plasma. The information derived from the knowledge of kinetic energies of the fragment ions is important for constructing potential energy curves that perturb the stable electronic states and cause predissociation. Therefore an accurate knowledge of these energies is of fundamental importance.

Studies on the kinetic energies of the fragment ions first began when Condon (36) predicted that the 30 eV energy loss in H_2 was not due to the reaction $H_2 \Rightarrow H^+ + H^+$ but due to $H_2 \Rightarrow H + H^+ +$ kinetic energy. This was verified, later on, simultaneously by Bleakney (37) and Tate and Lozier (38).

Obtaining accurate values of kinetic energies near the threshold of ionization is a very difficult measurement task due to low energy of ions. Therefore, these types of data are scarce.

CONCLUSIONS

In this article an effort has been made to familiarize the reader with various aspects of electron–atom or –molecule collisions that result in ion formation. The references provided here and references contained within these references give more detailed insight into this process.

BIBLIOGRAPHY

1. S. M. Younger and T. D. Mark, in T. D. Mark and G. H. Dunn (eds.), *Electron Impact Ionization,* New York: Springer-Verlag, 1985, p. 1.
2. S. M. Younger and T. D. Mark, in T. D. Mark and G. H. Dunn (eds.), *Electron Impact Ionization,* New York: Springer-Verlag, 1985, p. 24.
3. Y.-K. Kim et al., *J. Chem. Phys.* **106**: 1026, 1977.
4. W. Lotz, *Z. Phys.,* **206**: 205 (1967); see also *Z. Phys.,* **232**: 101, 1968.
5. D. Rapp, P. Englander-Golden, and D. D. Briglia, *J. Chem. Phys.,* **42**: 408, 1965.
6. F. J. De Heer and M. Inokuti, in T. D. Mark and G. H. Dunn (eds.), *Electron Impact Ionization,* New York: Springer-Verlag, 1985, p. 232.
7. J. R. Pierce, in *Theory and Design of Electron Beams,* 2nd ed., Princeton, NJ: Van Nostrand, 1954.
8. N. J. Mason and W. R. Newell, *Meas. Sci. Technol.,* **1**: 983, 1990.
9. K. Turvey, *Eur. J. Phys.,* **11**: 51, 1990.
10. M. A. Khakoo and S. K. Srivastava, *J. Phys. E.* **17**: 1008, 1984.
11. G. Csanak et al., Elastic Scattering of Electrons by Molecules, in L. G. Christophorou (ed.), *Electron-Molecule Interactions and Their Applications,* New York: Academic Press, 1984.
12. M. I. Ramanyuk and O. B. Shpenik, *Meas. Sci. Technol.,* **5**: 239, 1994.
13. J. Perrin, *C. R.,* **121**: 1130, 1895.
14. J. Perrin, *Nature,* **53**: 298, 1896.
15. J. Perrin, *Ann. Chem. Phys.,* **7** (11): 503, 1897.
16. K. Fujii and S. K. Srivastava, *J. Phys. B,* **28**: L559, 1995.
17. R. Boivin and S. K. Srivastava, *J. Phys. B: At. Mol. Opt. Phys.,* **31**: 2381, 1998.
18. M. V. V. S. Rao, I. Iga, and S. K. Srivastava, *J. Geophys. Res.,* **100**: 26421, 1995.
19. T. D. Mark, in T. D. Mark and G. H. Dunn (eds.), *Electron Impact Ionization,* Springer-Verlag, New York: 1985, p. 137.
20. S. K. Srivastava, A. Chutjian, and S. Trajmar, *J. Chem. Phys.,* **63**: 2659, 1975.
21. R. T. Brinkman and S. Trajmar, *J. Phys. E.,* **14**: 245, 1981.
22. S. Trajmar and D. F. Register, in I. Shimamura, and K. Takayanagi (eds.), *Experimental Techniques for Cross Section Measurements in Electron Molecule Collisions,* New York: Plenum, 1982. Also see J. C. Nickel et al., *J. Phys. E,* **22**: 730, 1989.
23. S. K. Srivastava, US Patent, *Apparatus and method for characterizing the mass transmission efficiency of a mass spectrometer,* Patent No. 4,973,840, 1990.
24. T. R. Hays et al., *J. Chem. Phys.,* **88**: 823, 1988.
25. H. Deutsch, K. Becker, and T. D. Mark, in *Proc. 20th ICPEAC,* 1997, p. WE088.
26. S. K. Srivastava and O. J. Orient, in K. Prelac (ed.), *Production and Neutralization of Negative Ions and Beams,* New York: American Institute Physics, 1984.
27. D. R. Crosley, in G. W. F. Drake (ed.), *Atomic, Molecular and Optical Physics Handbook,* New York: American Institute Physics Press, 1996.
28. H. F. Winters and M. Inokuti, *Phys. Rev. A* **25**: 420, 1982.
29. M. Goto et al., *Jpn. J. Appl. Phys.,* **33**: 3602, 1994.
30. H. M. Rosenstock et al., in *Physical and Chemical Data,* published by the American Chemical Society and the American Institute of Physics for the National Bureau of Standards, 1977, p. 6.
31. G. H. Wannier, *Phys. Rev.,* **90**: 817, 1953.
32. H. J. Grosse and K. H. Bothe, *Z. Naturforsch.,* **A23**, 1583, 1968.
33. O. J. Orient and S. K. Srivastava, *J. Phys. B:* **20**: 3923, 1987.
34. H. Deutch, K. Becker, and T. D. Mark, *Int. J. Mass Spectrum. Ion Proc.,* **167/168**: 503, 1997.
35. J. Franko and E. Daltabuilt, *Rev. Mex. Fis.,* **27**: 475, 1978.
36. E. U. Condon, *Phys. Rev.,* **35**: 1180, 1930.
37. W. Bleakney, *Phys. Rev.,* **35**: 658, 1930.
38. J. T. Tate and W. W. Lozier, *Phys. Rev.,* **39**: 254, 1932.

S. K. SRIVASTAVA
California Institute of Technology